Quasispherical fuel compression and fast ignition in a heavy-ion-driven X-target with one-sided illumination

Enrique Henestroza,[1] B. Grant Logan,[1] and L. John Perkins[2]
[1]*Lawrence Berkeley National Laboratory, Berkeley, California 94720, USA*
[2]*Lawrence Livermore National Laboratory, Livermore, California 94550, USA*

(Received 16 November 2010; accepted 28 January 2011; published online 9 March 2011)

The HYDRA radiation-hydrodynamics code [M. M. Marinak *et al.*, Phys. Plasmas **8**, 2275 (2001)] is used to explore one-sided axial target illumination with annular and solid-profile uranium ion beams at 60 GeV to compress and ignite deuterium-tritium fuel filling the volume of metal cases with cross sections in the shape of an "X" (X-target). Quasi-three-dimensional, spherical fuel compression of the fuel toward the X-vertex on axis is obtained by controlling the geometry of the case, the timing, power, and radii of three annuli of ion beams for compression, and the hydroeffects of those beams heating the case as well as the fuel. Scaling projections suggest that this target may be capable of assembling large fuel masses resulting in high fusion yields at modest drive energies. Initial two-dimensional calculations have achieved fuel compression ratios of up to 150X solid density, with an areal density ρR of about 1 g/cm^2. At these currently modest fuel densities, fast ignition pulses of 3 MJ, 60 GeV, 50 ps, and radius of 300 μm are injected through a hole in the X-case on axis to further heat the fuel to propagating burn conditions. The resulting burn waves are observed to propagate throughout the tamped fuel mass, with fusion yields of about 300 MJ. Tamping is found to be important, but radiation drive to be unimportant, to the fuel compression. Rayleigh–Taylor instability mix is found to have a minor impact on ignition and subsequent fuel burn-up. © *2011 American Institute of Physics*. [doi:10.1063/1.3563589]

I. INTRODUCTION

Fast ignition with heavy-ion beams has long been considered for heavy-ion fusion.[1–7] It would be desirable to minimize fuel compression energy using quasi-three-dimensional compression geometry, and use beam illumination for both fuel compression and ignition from the same side to simplify fusion chamber design as well as reduce required beam bending from an accelerator driver to the chamber. To explore this goal, a simple axisymmetric target with deuterium-tritium (DT) filling a metal case with a cross section in the shape of an X, called the "X-target" (Fig. 1), is investigated using two-dimensional hydrodynamic implosion calculations. A quasispherical pulsed-power target driven by a magnetic z-pinch has been considered with a similar cross section but requires much higher fuel compressions and implosion velocities to enable central hot-spot ignition.[8] Lower fuel compression of large DT fuel mass ($\sim$1 g) has been considered in the impact fusion scheme,[9] which requires a much larger beam energy (10–50 MJ). Section II below describes an initial X-target concept and the HYDRA code used. Section III presents findings relating to four proof-of-principle questions for the X-target which motivated this paper. (a) To what degree can the X-target metal case shape, and the expansion of that case in regions where the beams penetrate through it, help achieve quasi-three-dimensional spherical fuel compression? (b) Does radiation (apart from bremsstrahlung losses) play an important role during X-target fuel compression? (c) To what extent might Rayleigh–Taylor instabilities of the fuel-case interface cause fuel-metal mixing affecting the ignition zone? (d) Assuming a step-wise pulse shaping in compression beam power, how many power steps (successive shocks) are required to achieve the desired fuel densities for fast ignition in the X-target geometry?

For initial proof-of-principle, and to simplify the requirements for an X-target accelerator driver, questions (a)–(d) above have been investigated assuming a single ion energy and mass (chosen to be 60 GeV U) for both fuel compression and ignition. Different beam pulse durations incident on the target are assumed to be provided by different degrees of drift compression (different head-to-tail velocity ramps $\delta v_z/v_z$ impressed on different beams drift compressing between a multibeam accelerator and the target); the ion energy of 60 GeV is in the middle of the range previously considered for heavy-ion fast ignition.[3] Potential accelerator drivers to produce the X-target ion beams, and how such accelerators might provide the shorter pulses and smaller focal spots needed for fast ignition, are beyond the scope of this paper. However, Refs. 2–7 describe some driver and focusing examples to consider. Provided suitable sources of high-charge-state heavy ions can be obtained, it can be noted that 60 GeV linac drivers using U^{+12} ions would have comparable voltage (5 GV) and length ($\sim$3 km) as linac drivers with 4 GeV singly charged heavy ions for indirect drive hohlraum targets.[10]

As this paper is focused on the fundamental (proof-of-principle) questions stated above for the X-target concept, considerable future work is anticipated, to be partly described in Sec. IV where we discuss the one-dimensional (1D) compression requirements for higher peak density ($\rho > 100$ g/cm^3), and in the conclusions, Sec. V.

 © 2011 American Institute of Physics

Author complimentary copy. Redistribution subject to AIP license or copyright, see http://php.aip.org/php/copyright.jsp

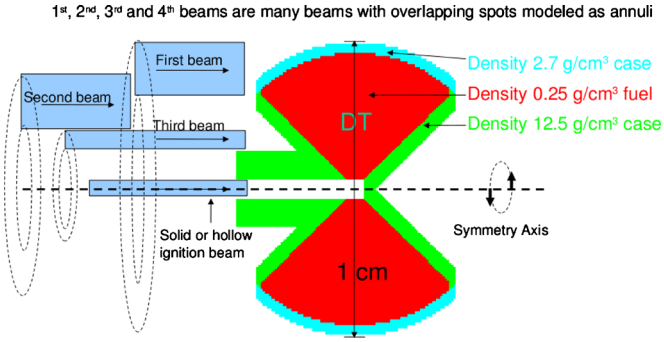

FIG. 1. (Color online) The X-target.

II. X-TARGET AND HYDRA CODE DESCRIPTION

Figure 1 shows the X-target geometry as used in the hydrodynamics code HYDRA, and Fig. 2 shows the location and energy depositions of the three annuli of heavy-ion beams used for compression [Figs. 2(a)–2(c)] as well as the solid central beams (overlapping on axis) used for ignition [Fig. 2(d)]; each frame corresponds to the initial time when each beam is injected. The color scheme corresponds to deposition energy per unit mass, which enhances the deposition at low densities to make the ion deposition distributions more noticeable. The material boundaries between the cases and the DT fuel are represented as black curves. The geometrical scale is the same as in Fig. 1.

The target geometry, as shown in Fig. 1, is obtained by removing two 45° half-angle cones from opposite sides of an otherwise spherical DT ball. This X-shaped fuel is enclosed in a metal case made of high density materials (2.5–20 g/cm^3). As an example, the outer (spherical) part of the case is chosen to be a density of 2.7 g/cm^3 metal (e.g., aluminum), and the side walls are chosen to be a density of 12.5 g/cm^3 metal (e.g., rhodium); target fabrication considerations are beyond the scope of this work, but lower-cost, higher-density high-Z case materials like lead or tungsten would be envisioned for future work. Also, in order to isolate the region where the ignition beam will pass, the upstream side of the case is made thicker to block the plasma blown off by the compression beams, and a channel is provided to allow the ignition beam to reach the vertex of the X-target.

The cylindrical heavy-ion beams are deposited in the outer case and DT fuel such that the X-target cone geometry transforms the effective cylindrical energy deposition into quasispherical fuel convergence. Thus, a key issue is the degree that we can approach ideal 1D spherical geometry in terms of final fuel stagnation densities. However, we note that because this target is ignited by a separate fast ignition beam, the usual constraints of low-mode symmetry and high-mode stability that attend conventional central hotspot ignition targets[11] are considerably relaxed. In particular, the adequacy of low-mode symmetry will be determined primarily by that required to achieve stagnation densities that approaches some reasonable fraction of ideal 1D values. (See Sec. IV for comparison with ideal 1D spherical geometries.)

The ion beams used to compress the fuel are three annuli of uranium beams with increasing power and energy. Energies of 0.5 and 1.5 MJ and pulse lengths of 25 ns, respectively, are used for the first and second compression beams and 1 MJ at 1 ns for the third beam. The total annular widths of the first and second beams are 1.4 mm, and 0.7 mm for the annular width of the third beam. The location of the compression beams is shown in Figs. 2(a)–2(c). The deposited beam energies in the metal case and in the fuel by these annular beams are manipulated by selecting the case material, thickness, and shape to create quasispherical "pistons" which hydrodrive a quasispherical fuel compression with low convergence (<5), without the need for significant radiation drive. Notice that the larger the case thickness and density, the better the tamping for pressures and hydrotimes; yet thinner and less dense cases would minimize beam loss through the case and provide more homogeneous energy deposition. For a given ion energy, the material composition through which the ion beam propagates has to be chosen appropriately; e.g., for the first compression beam, one would like to have a uniform energy deposition on the spherical cap to produce a uniform pressure, which requires moving the Bragg peak away from the target; but for the ignition beam, one would like to deposit all the beam energy in the DT, and therefore to have the Bragg peak inside the assembled fuel.

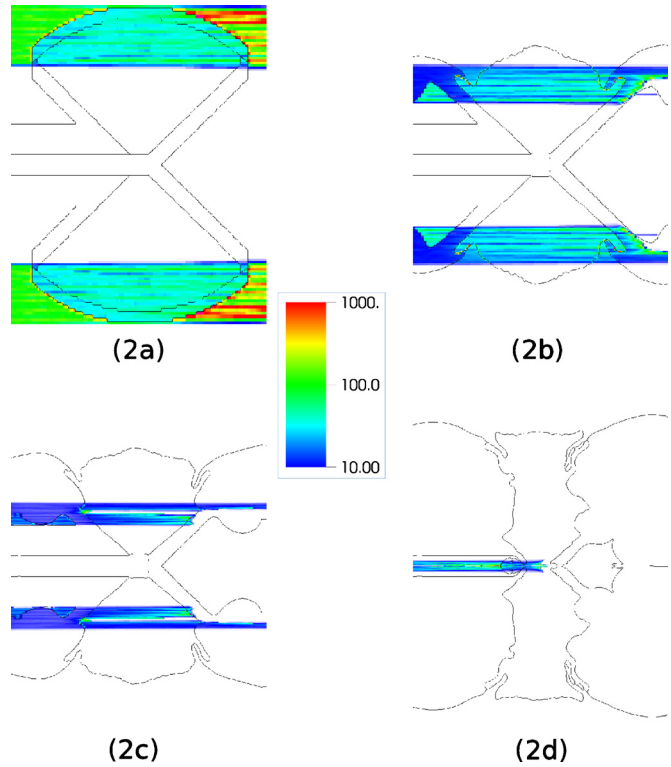

FIG. 2. (Color online) [(a)–(d)] Location of compression annular beams showing specific beam energy deposition distributions (arbitrary units) and material interfaces (black lines) at the beginning of each pulse. (a) First compression beam annulus. (b) Second compression beam annulus. (c) Third compression beam. (d) shows the ignition beam deposition at peak compression density; notice that the beam stops inside the fuel region.

As shown in Fig. 2(d), at full compression, an "ignition" annular or solid beam (assumed to be delivered by several overlapping beams on axis) is injected into the channel through the case on axis to heat the fuel to thermonuclear

Author complimentary copy. Redistribution subject to AIP license or copyright, see http://php.aip.org/php/copyright.jsp

conditions and start burn propagation. The energy of the ignition beam ranges between 1.0 and 3.0 MJ, the pulse length is 50–100 ps, and the beam radius is about 200 μm. HYDRA was used first to benchmark fast ignition calculations of isolated spherical balls of DT at densities between 50 and 300 g/cm^3, with results similar to Refs. 4 and 5. Based on these results, an ignition beam ion energy of 60 GeV was chosen as a compromise between fuel deposition energy and coupling efficiency through the case. Furthermore, to minimize the complexity of accelerator drivers for X-targets, the ion energy of the compression beams is also chosen to be 60 GeV.

Full radiation-hydrodynamics calculations including thermonuclear burn were performed with the HYDRA code.[12] The state of the art code HYDRA is a single-fluid, multiblock, multimaterial arbitrary-Lagrange-Eulerian radiation-hydrodynamics code. It runs in either two-dimensional (2D) or three-dimensional (3D) on a block-structured mesh of arbitrary quadrilaterals or hexahedrons, respectively. HYDRA treats radiation transport with multigroup radiation diffusion or implicit Monte Carlo photonics. Flux-limited electron and ion heat conduction are available. Thermonuclear burn is treated, as is the transport and deposition of energetic charged particles produced by thermonuclear reactions.

The simulation effort was based on 2D (RZ) calculations assuming axisymmetric target and annular and solid beams. Target fabrication errors and beam aiming errors can produce small sources of 3D effects. 3D effects can also be produced by the fact that the annular beams may be composed of individual solid beams located in a ring pattern, which breaks the assumption of rotational symmetry. On the other hand, the fuel convergence is small, less than 7 in the X-target, which minimizes the effect of nonaxisymmetric features. 3D simulations using HYDRA are planned for the compression phase to validate the assumption of cylindrical symmetry used here to treat the ring of ion beams as annular beams.

III. FINDINGS REGARDING THE BASIC PRINCIPLES OF THE X-TARGET CONCEPT

A. X-target metal case shape

The influence of the shape of the X-target case on the compression dynamics can be seen by comparing the density profiles for two instances. Figures 3(a) and 3(c) show the target geometry and density maps before the first compression beam is injected and Figs. 3(b) and 3(d) before the injection of the second compression beam. Figures 3(a) and 3(b) correspond to the case where the beam deposits its energy only in the DT. A dramatic change is obtained by placing a high density material in the beam path in such a way that the beam will deposit a large amount of energy at the entrance and exit of the DT region generating two axial pistons which convert the cylindrical into a quasispherical pressure profile.

In a similar way, a spherical piston can be generated by replacing the cylindrical cap in Fig. 3(c) by a spherical cap, as in the base case shown in Fig. 2(a). The ion beam deposits a larger energy per unit volume in the metallic spherical cap

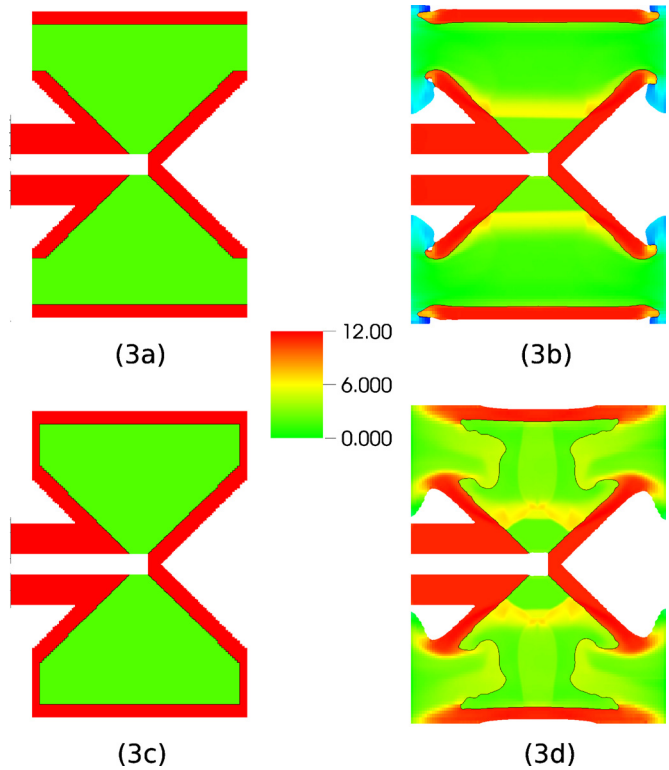

FIG. 3. (Color online) [(a)–(d)] Example of conversion of a cylindrical implosion into a quasi-three-dimensional (hemispherical) convergent implosion. Density profiles (g/cm^3) for (a) beam annulus going through case opening, (b) a cylindrical shock is launched. (c) Beam annulus depositing energy in the case, (d) a spherical shock is launched.

as compared to the energy per unit volume deposited in the low-density DT, thereby producing a high pressure region with spherical symmetry which compresses the DT fuel.

The thickness of the side walls (the X) should be enough to withstand the high pressure generated by the compressed fuel. Side walls of thickness less than 500 μm are observed to expand too rapidly to allow the DT fuel to be compressed quasispherically.

B. Radiation effects during X-target fuel compression and ignition

The influence of radiation during the compression phase in the X-target is quite small since the ion temperatures reach values under 100 eV. It is only at the final stage of compression (about 1 ns before the ignition beam is injected) that the temperature increases to a couple of hundred electron volts. Figure 4 shows the snapshots of the radial density profiles at the midplane of the X-target during the compression phase and at various times, when radiation effects are turned on and off. Notice that the influence of radiation on the density profiles is minor, i.e., the hydrodynamics is dominant.

C. Rayleigh–Taylor mix

The degree to which the Rayleigh–Taylor instabilities of the fuel-case interface cause fuel-metal mixing in the ignition zone can be seen in Fig. 5, which shows the material distribution at a time just before the injection of the ignition

Author complimentary copy. Redistribution subject to AIP license or copyright, see http://php.aip.org/php/copyright.jsp

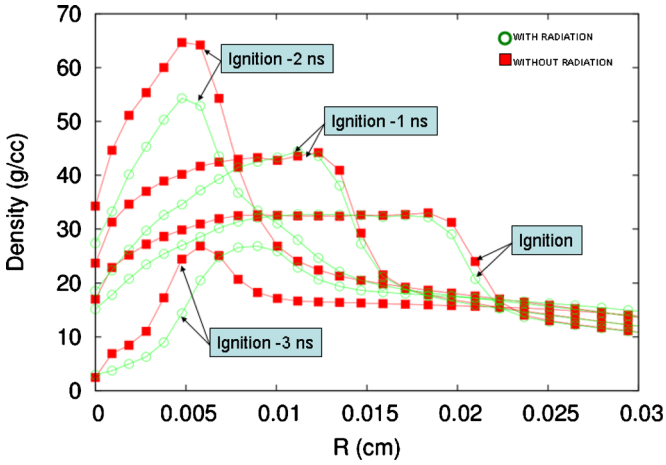

FIG. 4. (Color online) Radial density profiles at the midplane of the X-target as calculated by HYDRA with and without radiation at various times close to the ignition time.

beam. Even when there are some metal regions embedded in the DT fuel region, the impact on ignition and burn-up is minimal, since the regions of accumulated fusion yield occur well outside the mix region near the walls, and by the fact that the calculated burn fraction is given approximately by the standard formula $\rho R/(\rho R+7)$.

D. Fuel compression by a series of shocks generated by the ion beams

The maximum density of the assembled fuel can be achieved by compressing the fuel isentropically. Self-similar solutions[13] for isochoric implosion of solid density spherical shells at rest require a careful tailoring of the beam power delivered on the target. For one-sided axial target illumination with annular ion beams, we cannot provide such power profile. In this case, we are constrained to use a succession of 1, 2, or 3 compression beams for the X-target; the horizontal annuli of compression beams increase in power and energy, and decrease in radius. It is found that the series of shocks achieve peak DT fuel compression densities of 6, 20, and 30 g/cm^3, respectively, in the X-target geometry; these compression ratios are consistent with Guderley's solution for converging shock waves.[14] The beam positions and timing can likely be further optimized using a 1D analysis as a guide, as described in Sec. IV.

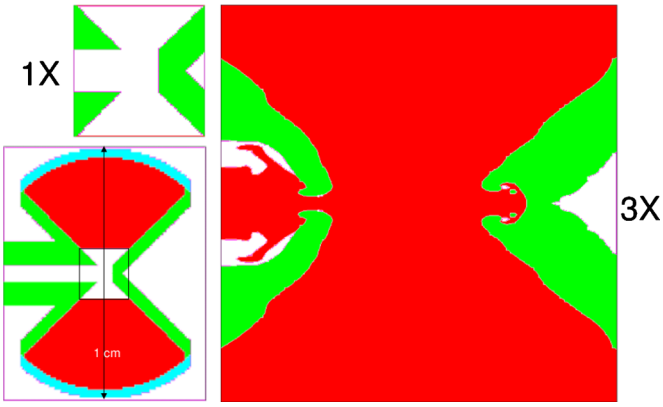

FIG. 5. (Color online) Material distribution at a time just before the injection of the ignition beam. The insets show the X-target and the zoomed region at the start of the HYDRA calculation.

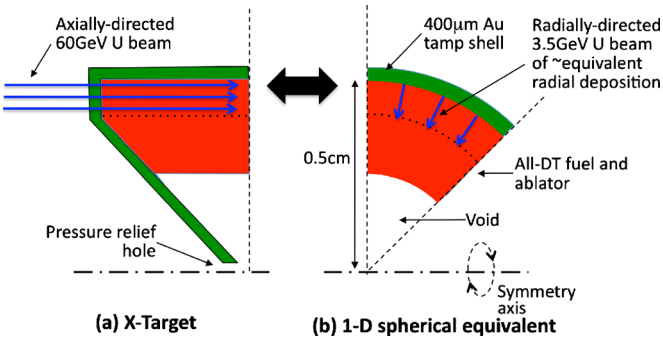

FIG. 6. (Color online) 1D spherical equivalent geometry of the X-target used to determine candidate target builds and drive dynamics for higher-density fuel assembly.

IV. ONE-DIMENSIONAL ANALYSIS OF FUEL COMPRESSION TO HIGHER DENSITIES

The initial 2D analysis summarized above is intended as proof-of-principle simulations of this new target concept without endeavoring to optimize implosion dynamics or ultimate performance. To commence this optimization process, we have performed an initial scoping study in spherical 1D geometry with the LASNEX radiation-hydrodynamics code[15] to determine candidate target build geometries and appropriate heavy-ion (HI) beam drive dynamics that result in higher-density assemblies. In Fig. 6(a), we show the X-geometry as analyzed in 2D above, and in Fig. 6(b) we show the 1D spherical equivalent of the X-target. Of course, compared to the X-target, the latter is an ideal spherical geometry but enables rapid optimization of candidate configurations (radial builds and driver pulse shapes) to be evaluated in the hydrocode. We then expect the X-target to approach the ideal 1D compression densities to a level determined by the real 2D perturbation in that quasispherical system. Further approach to the 1D stagnation densities may be attainable in the full configuration either with modest increases in drive energies and/or somewhat reduced fuel masses.

As shown in Fig. 6(b), the all-DT fuel plus ablator is arranged as a low-aspect-ratio, thick spherical shell inside an Au tamper shell. In the 2D geometry of the X-target, the 60 GeV U annular beams are directed axially across the ablator. In the 1D spherical equivalent of Fig. 6(b), the HI source originates on the inside of the tamp shell and is directed radially inward as shown. Given that we require around the same equivalent radial deposition in the ablator, we must reduce the beam kinetic energy to ~3.5 GeV corresponding to an areal range of ~0.035 g/cm^2 or a linear range of ~0.14 cm.

Because the outward expansion of the ablator is constrained by the Au shell, the tamped ablation acts analogous to that of a cannon rather than that of the freely expanding rocket ablation of conventional Inertial Confinement Fusion (ICF) targets. Correspondingly, higher drive efficiencies are

Author complimentary copy. Redistribution subject to AIP license or copyright, see http://php.aip.org/php/copyright.jsp

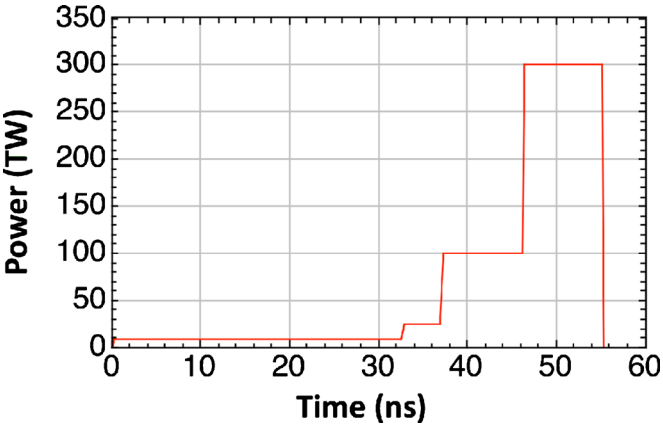

FIG. 7. (Color online) Heavy-ion pulse shape for fuel assembly. The total energy and peak powers are 4 (2) MJ and 300 (150) TW, respectively, for a full (half) sphere.

TABLE I. Results of initial LASNEX fuel assembly simulations in 1D spherical geometry. The values in parentheses for extensive quantities are those corresponding to an ideal spherically converging X-target with a 45° half-angle, which is 50% of the full-sphere values.

Fuel mass	35.2 (17.6) mg
Fuel inner radius and radial thickness	0.24 cm, 0.120 cm
Ablator radial thickness	0.140 cm
Heavy-ion drive energy for compression	4 (2) MJ
Peak drive power	300 (150) TW
Maximum areal density ρ-R	3.38 g/cm^2
Peak fuel density at max ρ-R	101 g/cm^3
Average fuel density at max ρ-R[a]	83.3 g/cm^3
Approximate projected fusion yield[b]	~3.8(1.9) GJ

[a]Density radially averaged over the shell between the 1/e of peak density points.
[b]Yield of this assembled fuel mass assuming an appropriate ignition source and a burn fraction of $\sim\rho R/(\rho R+7)$.

attainable. The thickness of the tamp shell (400 μm) is determined by the transit time of the pressure shock to the outer surface relative to the end of the HI drive pulse. As the X-target is configured with a pressure relief hole to enhance late time convergence, we stipulate a void inside the fuel rather than the conventional 0.3 mg/cm^3 equilibrium vapor pressure of solid DT fuel.

We then deduce the required radial build and HI drive dynamics by requiring (a) an ingoing fuel mass that would give a fusion energy yield of 3 (1.5) GJ at a nominal burn fraction of 25%, (b) an ablator radial thickness of 0.14 cm corresponding to a typical X-target annular beam thickness, (c) an initial fuel aspect ratio of 2.5 to provide good in-flight stability (low in-flight-aspect-ratio), (d) an outer maximum diameter of 1 cm, and (e) a total HI drive energy of 4(2) MJ for the fuel compression only. The corresponding fuel mass is then 35.2 (17.6) mg, and the ratio of fuel, i.e., payload, mass to total initial mass is ~0.3. (In this section where we quote extensive quantities, e.g., energies, masses, etc., the values in parentheses are those corresponding to an ideal spherically converging X-target with a 45° half-angle, and are therefore 50% of those of the full-sphere values. Intensive quantities, e.g., densities, etc., are, by definition, the same.)

The heavy-ion beam pulse shape for fuel assembly is shown in Fig. 7. The foot power of 8.2 (4.1) TW is set to provide an average tamped ablation pressure of ~1 Mbar over its duration, while the 300 (150) TW peak power and the start of its rise is optimized to maximize the final assembled areal density (ρR) of the fuel subject to the 4 (2) MJ total energy constraint above. The intermediate power pedestals are timed to synchronize shock breakout with the foot shock on the inside of the fuel. This is a three-shock plus main pulse shape. A four-shock plus main pulse shape can result in ~7% higher areal densities due to more precise tuning of the adiabat, while more than four initial pedestals result in little or no increased benefit to late time assembly.

Initial results are shown in Table I. Given the efficient tamped ablation drive, large fuel masses can potentially be assembled in this target platform. In particular, we note the possibility for obtaining peak densities in excess of 100 g/cm^3 and assembled areal densities of ~3.5 g/cm^2 for fuel masses of ~35(17) mg. If appropriately ignited with a separate fast ignition energy source, this offers the prospects for gigajoule fusion yields and target gains of several-hundreds at modest drive energies. As was described above, this happens in ideal spherical geometry but such densities should be approachable in the full configuration either with modest increases in drive energies and/or somewhat reduced fuel masses.

V. CONCLUSIONS

A succession of three horizontal annuli of compression beams at increasing powers and energies, and at decreasing radii, is found to be needed to achieve peak DT fuel compression densities of 6, 20, and 30 g/cm^3, respectively, in the X-target geometry. To reduce the required heavy-ion beam ignition energy below the current level of 3 MJ at peak density of 30 g/cm^3, work in progress is seeking to achieve fuel densities of >100 g/cm^3 (fuel convergence increases from 5 to >7) and with improved beam-into-fuel coupling efficiencies (from currently low levels of 20% to above 40%). As indicated in Sec. IV, 1D implosion analysis suggests at least one additional compression drive pulse might be needed to reach peak $\rho>100$ g/cm^3, one more than the three used in this report.

The results presented here are intended as initial examples reaching sufficient fuel compression (~200X solid DT) to provide a proof-of-principle for this novel fuel assembly and heavy-ion drive geometry. Already, these X-target results give target performance comparable to that of indirect drive heavy-ion targets.[10] The X-target design is far from optimized and many further improvements can be envisioned. The results of these first examples give confidence that by careful tailoring of all the available parameters, DT fuel with a density of >50 g/cm^3 and $\rho r>2$ g/cm^2 should be achievable. If so, this target platform should be capable of assembling large fuel masses resulting in high fusion yields at modest heavy-ion drive energies.

Author complimentary copy. Redistribution subject to AIP license or copyright, see http://php.aip.org/php/copyright.jsp

In particular, improvements can be expected in the beam deposition and coupling efficiency into DT by optimizing the ion kinetic energy together with the X-target case thicknesses. The third compression beam annulus, as well as using hollow ignition beams,[16,17] might be explored with higher power levels at shorter pulses of a few hundred picoseconds, attempting to shock compress densities of 20 g/cm^3 at the end of the second compression pulse to >100 g/cm^3 before the final ignition pulse. The shape of the ignition beam (solid to hollow), consisting of several overlapping individual beam spots, and focused in a more convergent geometry, might be further optimized together with the shape of the fuel at stagnation and with the shape of a semicavity hydroformed into the compressed case near the vertex to reduce ignition energy and lengthen ignition pulses to more than 100 ps.

Burn waves ($T_{ion} \sim 15$ keV) have already been observed in this work to begin propagating radially outward into the lower density regions of the X-target, much like the asymmetric hemispherical target proposed by Nuckolls[18] for gain 1000. To the extent future work succeeds in achieving higher ρ and $\rho r > 2$ g/cm^2, a much larger fusion yield contribution from burn waves propagating into the outer low-density fuel region of the X-target may lead to lower drive energy, larger fusion yields of 1–2 GJ, and much higher gains.

ACKNOWLEDGMENTS

This work was in part inspired by discussions with Boris Sharkov (the application of axisymmetric beam annular compression drive exploiting beam spot rotation using R. F. "wobblers") and by discussions with John Nuckolls (encouraging the exploration of fast ignition of lower density fuel assemblies for higher gain using heavy-ion beams).

This work was performed under the support of the U.S. Department of Energy by the Lawrence Berkeley National Laboratory under Contract No. DE-AC02-05CH11231 and the Lawrence Livermore National Laboratory under Contract No. DE-AC52-07NA27344.

[1] A. W. Maschke, Proceedings of the 1975 IEEE Particle Accelerator Conference, 1975, p. 1875; IEEE Report No. NS-22, June 1975.
[2] M. Tabak, J. Hammer, M. E. Glinsky, W. L. Kruer, S. C. Wilks, J. Woodworth, E. M. Campbell, M. D. Perry, and R. J. Mason, Phys. Plasmas **1**, 1626 (1994).
[3] M. Tabak and D. A. Callahan-Miller, Proceedings of the 12th International Symposium on Heavy Ion Inertial Fusion, Heidelberg, Germany, 24–27 September 1997; [Nucl. Instrum. Methods Phys. Res. A **415**, 75 (1998)].
[4] M. Temporal, J. J. Honrubia, and S. Atzeni, Phys. Plasmas **9**, 3098 (2002).
[5] S. A. Medin, M. D. Churazov, D. G. Koshkarev, B. Yu. Sharkov, Yu. N. Orlov, and V. M. Suslin, Laser Part. Beams **20**, 419 (2002).
[6] B. G. Logan, R. O. Bangerter, D. A. Callahan, M. Tabak, M. Roth, L. J. Perkins, and G. Caporaso, Fusion Sci. Technol. **49**, 399 (2006).
[7] D. A. Callahan-Miller and M. Tabak, Phys. Plasmas **7**, 2083 (2000).
[8] T. Nash, P. VanDevender, N. Roderick, and D. McDaniel, Sandia National Laboratories Report No. SAND2007-7178, November 2007.
[9] S. Kawata and T. Saitoh, Proceedings of the Tenth International Conference on High Power Particle Beams, 1994, p. 179.
[10] S. S. Yu, W. R. Meier, R. P. Abbott, J. J. Barnard, T. Brown, D. A. Callahan, C. Debonnel, P. Heitzenroeder, J. F. Latkowski, B. G. Logan, S. J. Pemberton, P. F. Peterson, D. V. Rose, G.-L. Sabbi, W. M. Sharp, and D. R. Welch, Fusion Sci. Technol. **44**, 266 (2003).
[11] J. Lindl, Phys. Plasmas **2**, 3933 (1995).
[12] M. M. Marinak, G. D. Kerbel, N. A. Gentile, O. Jones, D. Munro, S. Pollaine, T. R. Dittrich, and S. W. Haan, Phys. Plasmas **8**, 2275 (2001).
[13] D. S. Clark and M. Tabak, Nucl. Fusion **47**, 1147 (2007).
[14] G. Guderley, Luftfahrtforschung **19**, 302 (1942).
[15] G. B. Zimmerman and W. L. Kruer, Comments Plasma Phys. Controlled Fusion **2**, 51 (1975).
[16] M. Herrmann, S. Hatchett, and M. Tabak, Bull. Am. Phys. Soc. **46**, 106 (2001).
[17] M. Temporal, R. Ramis, J. J. Honrubia, and S. Atzeni, Plasma Phys. Controlled Fusion **51**, 035010 (2009).
[18] J. H. Nuckolls, J. Phys.: Conf. Ser. **244**, 012007 (2010).

Author complimentary copy. Redistribution subject to AIP license or copyright, see http://php.aip.org/php/copyright.jsp